JOURNAL OF SOLID STATE CHEMISTRY **135,** 96–102 (1998)
ARTICLE NO. SC977602

XRD and Solid-State NMR Study of Magnesium Oxide–Magnesium Orthophosphate Systems

Maria Angeles Aramendía, Victoriano Borau, César Jiménez,[1] José Maria Marinas, Francisco José Romero, and José Rafael Ruiz

Department of Organic Chemistry, Faculty of Sciences, Córdoba University, Av. San Alberto Magno s/n, E-14004 Córdoba, Spain

Received March 7, 1997; in revised form August 15, 1997; accepted August 19, 1997

Various magnesium oxide–magnesium orthophosphate systems in different Mg/P ratios were synthesized and examined by XRD and ^{1}H and ^{31}P MAS NMR. The results thus obtained are compared with those for commercially available pure MgO and $Mg_3(PO_4)_2$. The crystallization temperature of magnesium orthophosphate was found to increase with increasing MgO content in the sample. The NMR technique revealed the absence of interactions between the two species. ^{31}P MAS NMR allowed the amorphous-to-crystalline ratio for magnesium orthophosphate in solids calcined at different temperatures to be determined. Also, ^{1}H MAS NMR revealed the qualitative nature of hydroxyl sites in the solids. © 1998 Academic Press

INTRODUCTION

The literature on the use of metal orthophosphates as catalysts for organic processes grows day by day. Thus, $AlPO_4$ (1–4), $BiPO_4$ (5–7), BPO_4 (8), $FePO_4$ (9), Li_3PO_4 (10), and $Mg_3(PO_4)_2$ (11) have been used in organic syntheses involving catalysis by acid or acid and basic sites. Magnesium orthophosphates have not yet been fully explored as catalysts for organic processes, however. Our group has used various magnesium orthophosphates obtained by modified synthetic procedures in the gas-phase dehydration–dehydrogenation of cyclohexanol (12).

In recent years, solid-state NMR spectroscopy has grown enormously in use for characterizing solids, in combination with diffraction techniques for examining crystalline phosphates. Also, solid-state NMR spectroscopy has become a crucial tool for identifying amorphous compounds, which is unaffordable by X-ray diffraction techniques, as it allows the local environment of atoms with a potential catalytic activity to be characterized.

Because characterizing the chemical nature and properties of surface active sites is one of the main goals of catalysis research, authors have used a variety of physical techniques including IR, visible, UV, and Raman spectroscopies, in addition to ESR, ESCA, EXAFS, and XRD, among others, for this purpose. Specifically, ^{1}H MAS NMR spectroscopy was recently used for the structural elucidation of Al_2O_3 (13), TiO_2–SiO_2 (14), and V_2O_5–$AlPO_4$ systems (15). Also, ^{31}P MAS NMR has enabled the characterization of the local environment of phosphorus atoms in both amorphous and crystalline phosphates (16–19).

This work reports on the synthesis and characterization of magnesium oxide–magnesium orthophosphate systems by use of various instrumental techniques. The results thus obtained are compared with those for commercially available magnesium oxide and magnesium orthophosphate.

EXPERIMENTAL

Materials

The magnesium oxide–magnesium orthophosphate systems studied in this work are designated $Mg_{100-x}P_x$, where x is the percent mole fraction of magnesium phosphate and $100 - x$ that of magnesium oxide in the solid. Thus, the solid named $Mg_{50}P_{50}$ was obtained by dropwise addition of a solution containing 8.6 ml of H_3PO_4 ($\rho = 1.8\,g/cm^3$) in 50 ml of distilled water over a suspension of 22.2 g of $Mg(OH)_2$ in 50 ml of distilled water in an ice bath under continuous stirring that was extended for a further 1 h after addition was finished. The resulting suspension was vacuum-dried. Solids $Mg_{25}P_{75}$ and $Mg_{75}P_{25}$ were obtained by the same procedure but using 22.2 g of $Mg(OH)_2$ and 12.9 ml of H_3PO_4 for the former and 22.2 g of $Mg(OH)_2$ plus 4.3 ml of H_3PO_4 for the latter.

Solids MgP (Aldrich 34,470-2) and MgO (Probus 3225) were commercially available products of formula $Mg_3(PO_4)_2 \cdot xH_2O$ and $Mg(OH)_2$, respectively.

All solids were sieved through 200–250 mesh and dried in a stove at 293 K prior to calcination at 623, 773, 923, or 1073 K.

[1] To whom correspondence should be addressed.

0022-4596/98 $25.00

X-Ray Diffraction Analysis

X-ray diffraction (XRD) patterns were recorded on a Siemens D500 diffractometer using CuK_α radiation. Scans were performed over the 2θ range from 7° to 50°.

NMR Spectra

Solid-state ^1H and ^{31}P NMR spectra were recorded on a Bruker ACP-400 spectrometer at 400.13 and 161.975 MHz, respectively, at room temperature. Typical spinning speeds (3.5 kHz) were used with all samples. The excitation pulse and recycle time for ^1H NMR were 5 μs ($\pi/2$ pulse) and 1 s (1000 scans), respectively—longer delay times had little effect on the relative intensities of proton resonances. The excitation pulse and recycle time for ^{31}P NMR were 5 μs ($\pi/2$ pulse) and 3 s (300 scans), respectively. The contact time for the transfer of magnetization between protons and ^{31}P (CP experiments) was 10 ms (300 scans). ^1H and ^{31}P shifts were measured relative to tetramethylsilane and H_3PO_4, respectively. All samples were degassed to 3 μm Hg at 393 K for 8 h before their spectra were recorded.

RESULTS AND DISCUSSION

XRD Results

Figure 1 shows the XRD patterns for solid MgP heated at different calcination temperatures. The uncalcined solid exhibited bands consistent with the formula $Mg_3(PO_4)_2 \cdot 8H_2O$. As can be seen in the figure, the solid was amorphous at 393 and 623 K and exhibited some crystallinity above 773 K. The crystalline structure was identified as $Mg_3(PO_4)_2$ (farringtonite phase) over the temperature range 923–1073 K.

Figure 2 shows the patterns corresponding to solid MgO calcined at different temperatures. The uncalcined solid consisted of brucite $Mg(OH)_2$. On calcination at 623 K it exhibited primarily $Mg(OH)_2$ bands and incipient periclase MgO bands. At 773 K, the solid consisted virtually completely of periclase; also, brucite bands were almost absent from the patterns. Finally, at 923 and 1073 K, the solid consisted of highly crystalline periclase MgO.

Figure 3 shows the XRD patterns for magnesium oxide–magnesium orthophosphate in a $Mg_{50}P_{50}$ sample. All uncalcined solids exhibited the diffraction bands for brucite $Mg(OH)_2$ and $Mg_3(PO_4)_2 \cdot 22H_2O$. Calcination led to amorphization of all the solids; the band for periclase MgO was clearly observed above 773 K. The higher the proportion of magnesium oxide in the solid was, the stronger were these bands. Magnesium orthophosphate was amorphous in all solids except those treated at 923 K, where it appeared to be slightly crystalline. The pattern in Fig. 3c reveals that solid $Mg_{50}P_{50}$ calcined at 923 K was a mixture of periclase MgO and farringtonite $Mg_3(PO_4)_2$. Kanazawa *et al.* (20) reported the transition from $Mg_3(PO_4)_2 \cdot 22H_2O$ to $Mg_3(PO_4)_2 \cdot 8H_2O$ to occur at 328 K in a water-rich atmosphere. We could not identify such a transition or the phosphate octahydrate on raising the calcination temperature, although we cannot rule out its occurrence. It is logical to think that the octahydrate (whether crystalline or otherwise) may have been formed as the calcination temperature was raised in our case before the anhydrous magnesium orthophospate reached by subjecting the solids to high calcination temperatures appeared.

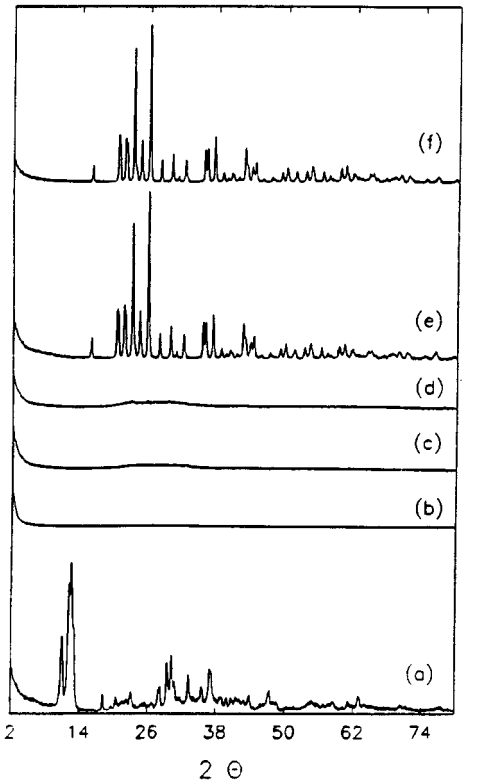

FIG. 1. XRD patterns for solid MgP, uncalcined (a) and calcined at 393 (b), 623 (c), 773 (d), 923 (e), and 1073 K (f).

The presence of MgO in different proportions in the solid had an appreciable effect on the thermal transformation of magnesium orthophosphate. The formation of interstitial MgO inhibits or delays—depending on the particular solid—the crystallization of $Mg_3(PO_4)_2$ species.

Uncalcined solids can be assumed to contain the species brucite $Mg(OH)_2$ and $Mg_3(PO_4)_2 \cdot 22H_2O$. When these solids are calcined at 773 K, the sole identifiable bands are those for periclase MgO on an amorphous background—in fact, magnesium orthophosphate is amorphous at that temperature. The orthophosphate bands were also hardly distinguishable in the patterns obtained on calcination at 923 K. It was shown elsewhere that magnesium

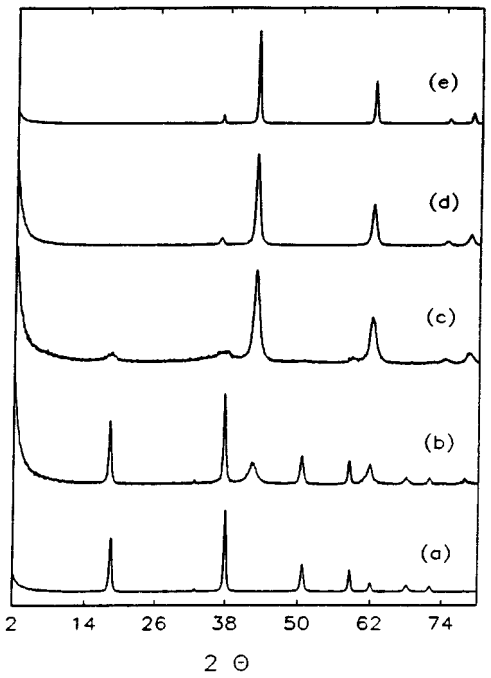

FIG. 2. XRD patterns for solid MgO, uncalcined (a) and calcined at 623 (b), 773 (c), 923 (d), and 1073 K (e).

orthophosphate changes from amorphous to crystalline below 923 K; consequently, the presence of MgO in these systems may delay the crystallization of amorphous magnesium orthophosphate.

^{31}P NMR Spectroscopy

Figure 4a shows the ^{31}P MAS NMR spectra for solid MgP calcined at different temperatures. As can be seen, the

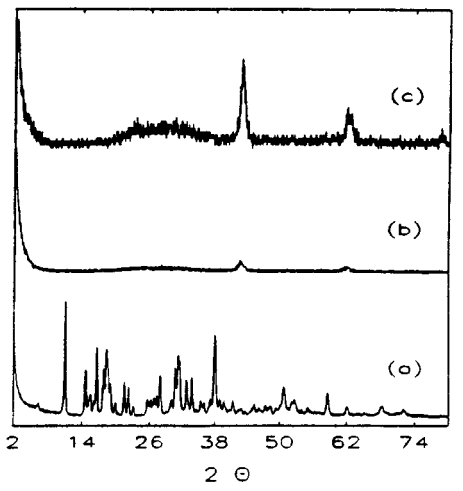

FIG. 3. XRD patterns for solid $Mg_{50}P_{50}$, uncalcined (a) and calcined at 773 (b) and 923 K (c).

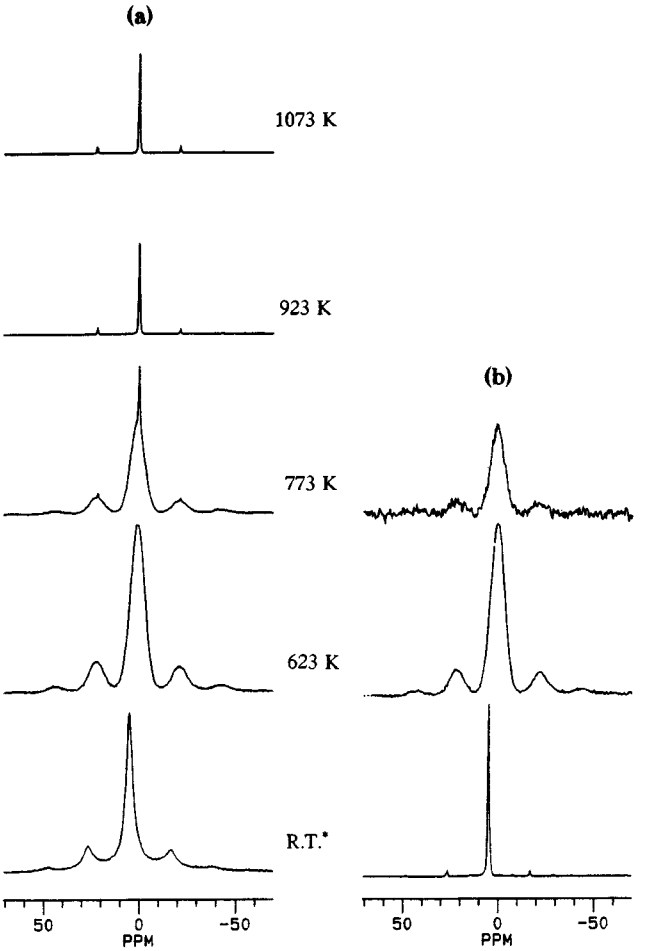

FIG. 4. ^{31}P NMR spectra for solid MgP, uncalcined and calcined at different temperatures: (a) MAS spectra; (b) CP/MAS spectra. *Room temperature.

spectra consist of a single component and a symmetric series of spinning sidebands (ssb). The behavior of this signal at different temperatures was consistent with previous XRD findings. Thus, the chemical shift and width for this component changed with the thermal treatment applied (Table 1) as a result of the conversion from a crystalline

TABLE 1

Chemical Shifts (in ppm Relative to 85% w/w H_3PO_4) and Widths of the Signals for Solid MgP Calcined at Different Temperatures

T (K)	δ ^{31}P (ppm)	ν (Hz)	Crystal phase
Room	4.6	732	$Mg_3(PO_4)_2 \cdot 8H_2O$
623	0.5	1463	Amorphous
773	0.5	1458	Amorphous
	− 0.5	134	Farringtonite
923	− 0.5	132	Farringtonite
1073	− 0.5	130	Farringtonite

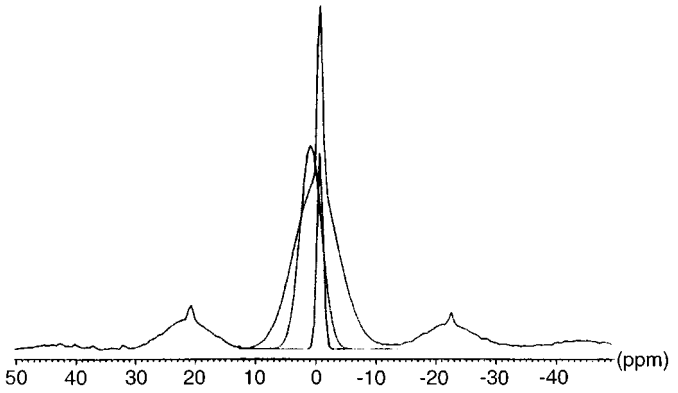

FIG. 5. ^{31}P MAS NMR spectrum of MgP calcined at 773 K together with its decomposition into Gaussian lines.

phase to an amorphous phase and back to a new crystalline phase. The spectrum for the uncalcined sample exhibited a chemical shift of 4.6 ppm that dropped to 0.5 ppm *on calcination* at 623 K. The spectrum for the sample calcined at 773 K exhibited two overlapped signals. It can be seen that the experimental line can be decomposed into two Gaussian lines (Fig. 5) with different line widths and chemical shifts (Fig. 4c), indicating the presence in this sample of two different types of ^{31}P nuclei, corresponding to the amorphous (0.5 ppm) and crystalline (farringtonite) magnesium orthophosphate (-0.5 ppm). This Gaussian deconvolution allowed the width, chemical shift, and area for each signal in this spectrum to be determined; in this way, the solid was found to be 76% amorphous and 24% crystalline. The solids calcined at 923 and 1073 K gave a sharp signal corresponding to farringtonite magnesium orthophosphate, consistent with a previous finding from the XRD patterns (Figs. 1d and 1e), which exhibited weak signals that strengthened as the calcination temperature was increased (to 923 K). These results suggest that the crystalline and amorphous phases of magnesium orthophosphate already coexist at 773 K. This was previously inferred from a SEM study (12) that revealed the presence of two types of particles: flat, oblong or in the shape of elongated rods.

To identify the phosphorus atoms bonded to OH groups, the ^{31}P CP/MAS spectra shown in Fig. 4b were recorded. In this technique, the polarization transfer from ^{1}H nuclei to

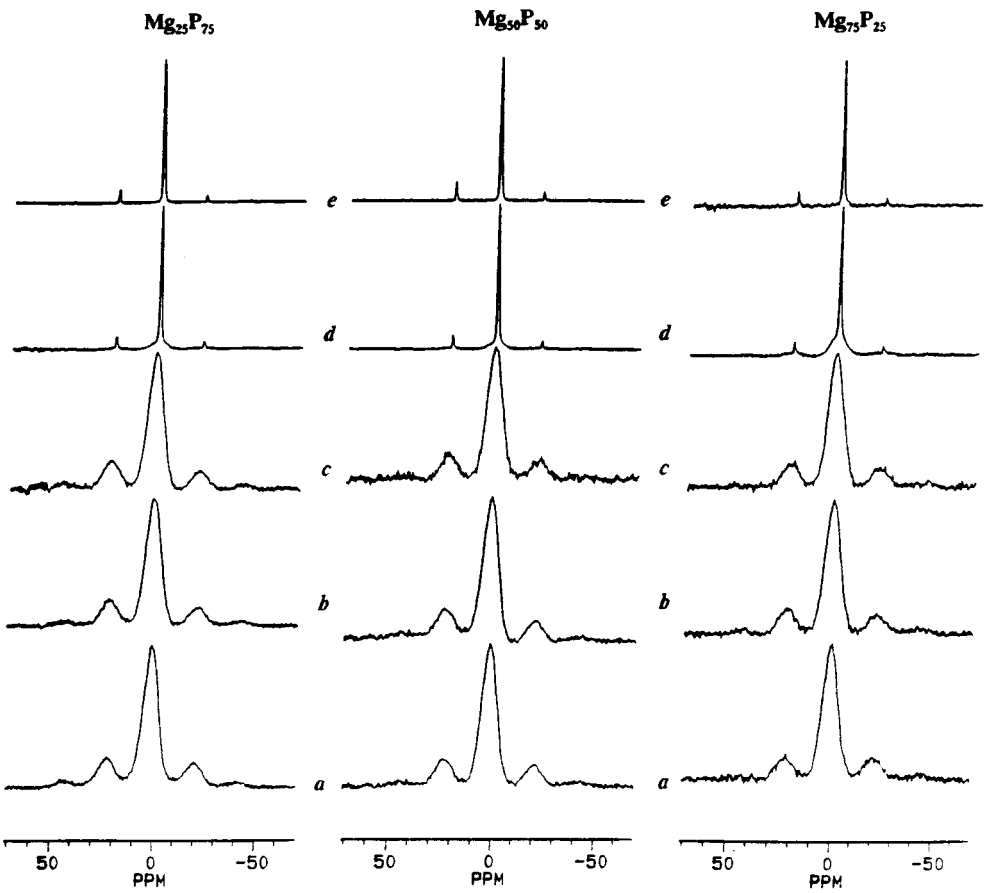

FIG. 6. ^{31}P MAS spectra for solid $Mg_{100-x}P_x$, uncalcined (a) and calcined at 623 (b), 773 (c), 923 (d), and 1073 K (e).

^{31}P nuclei takes place by irradiation of the two types of nuclei at their respective resonance frequencies under the Hartmann–Hahn condition (21, 22). Spinning the sample and irradiating the protons while the ^{31}P signal is acquired reduce ^{1}H–^{31}P dipole interactions and sharpens the phosphorus signal. The uncalcined sample exhibited a sharp signal (163 vs 732 Hz in the MAS spectrum) of greater height, which suggests the presence of OH groups bonded to phosphorus throughout the crystal lattice. As the calcination temperature was raised, the phosphorus signal decreased and eventually disappeared at 923 K by the effect of the sample dehydroxylation. The ^{31}P CP/MAS spectrum obtained at 923 K contained a single signal (0.5 ppm), thus indicating that it was the phosphorus in the amorphous phase that bonded to OH groups.

These results are quite consistent with those previously obtained by the X-ray technique. In fact, the solid was found to be crystalline at 923 and 1073 K, but amorphous at 623 K, where it exhibited no diffraction. The uncalcined solid was crystalline in nature [consistent with the formula $Mg_3(PO_4)_2 \cdot 8H_2O$] and exhibited very weak XRD signals at 773 K corresponding to farringtonite $Mg_3(PO_4)_2$ on an amorphous background.

Figure 6 shows the ^{31}P MAS NMR spectra for the magnesium oxide–magnesium orthophosphate system studied. Obviously, the intensity of the ^{31}P signal decreased with decreasing phosphorus content in the sample; however, the uncalcined sample always exhibited a signal at 1.1 ppm, which, consistent with the XRD results, can be ascribed to the phosphorus in $Mg_3(PO_4)_2 \cdot 22H_2O$. The signal for the solids calcined at 623 K appeared at 0.5 ppm, which suggests the transformation into an amorphous phase identical with that formed in solid MgP. However, in these systems, MgO increases the crystallization temperature because the three samples remained completely amorphous at 773 K—unlike pure MgP, which exhibited some crystallinity at that temperature. The crystalline phase was distinguishable in the samples calcined at 823 K; however, there was still some amorphous phase, the content of which increased with increasing magnesium content in the system. Table 2 gives the proportions of the two phases, calculated by Gaussian deconvolution of the spectra. Finally, calcination at 1073 K yielded crystalline magnesium orthophosphate (farringtonite phase) in every case ($\delta = -0.5$ ppm).

TABLE 2
Proportions of Amorphous and Crystalline Orthophosphate in $Mg_{100-x}P_x$ Systems Calcined at 923 K

Sample	% Amorphous	% Crystalline
MgP	0.0	100.0
$Mg_{75}P_{25}$	49.4	50.6
$Mg_{50}P_{50}$	27.1	72.9
$Mg_{25}P_{75}$	10.8	89.2

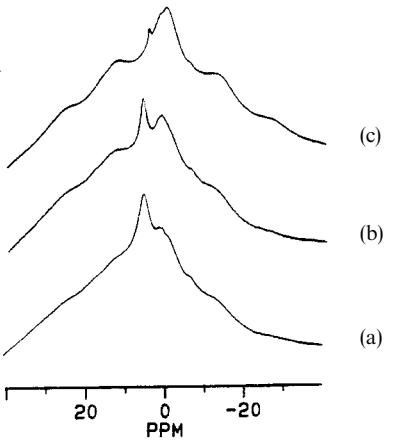

FIG. 7. ^{1}H MAS NMR spectra for solid MgO, uncalcined (a) and calcined at 623 (b), and 773 K (c).

^{1}H MAS NMR Spectroscopy

Owing to the dehydroxylation undergone by the solids studied on raising the calcination temperature, the ^{1}H MAS NMR study was carried out only on the solids that were pretreated in a stove at 393 K and those calcined at 623 and 773 K. The signals of the probe and rotor are negligible.

The spectrum for the uncalcined MgO solid (Fig. 7) exhibited two signals, centered at 5.2 and 1.2 ppm. The former, which was the stronger, based on its downfield shift, can be assigned to OH groups in $Mg(OH)_2$, where brucite layers are still hydroxylated. On the basis of the results of Brunet and Schaller (23), the signal centered at 1.2 ppm can

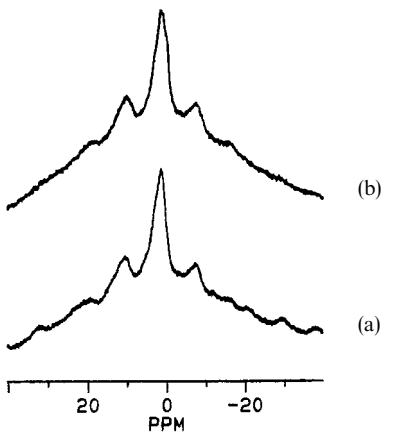

FIG. 8. ^{1}H MAS NMR spectra for solid MgP calcined at 623 (a), and 773 K (b).

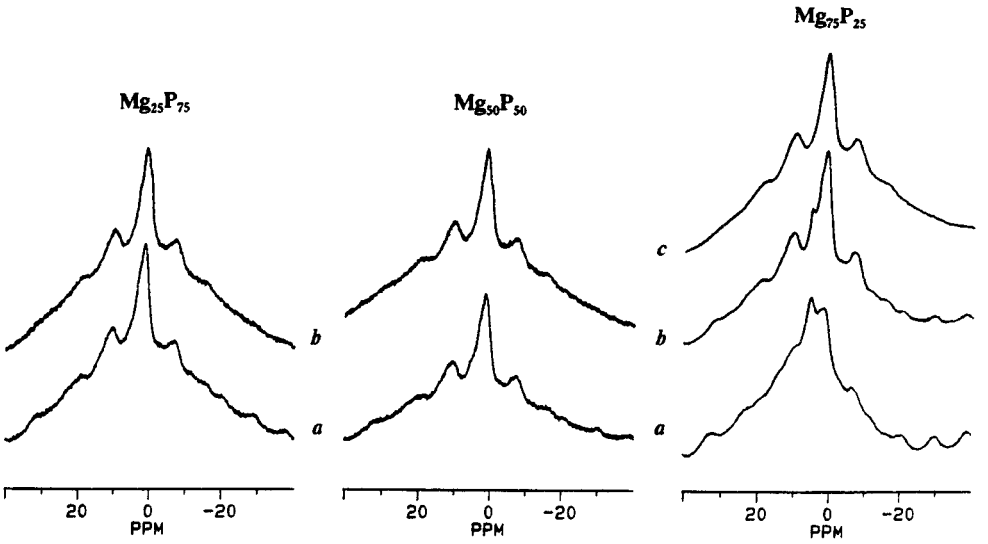

FIG. 9. ^1H MAS spectra for solid $Mg_{100-x}P_x$ calcined at 623 (a), 773 (b), and 923 K (c).

be assigned to hydroxyl groups bonded to the second layer of magnesium atoms. Calcining solid MgO at 623 K considerably decreased the signal at 5.2 ppm as a result of the partial dehydroxylation observed at that temperature, by which part of $Mg(OH)_2$ became MgO. Raising the calcination temperature to 773 K led to complete dehydroxylation of $Mg(OH)_2$, which was converted into periclase MgO; the spectrum contained three signals, at 3.6, 0.5, and -1.1 ppm, the last of which was the strongest and must correspond to "basic" OH groups, judging by its upfield shift. The signal at 0.5 ppm can be assigned to "less basic" OH groups. Finally, the downfield shift of the signal at 3.6 ppm suggests the presence of hydrogen bonds involving these surface hydroxyl groups.

Figure 8 shows the spectra for the MgP samples calcined at 623 and 773 K. The former contained two signals, centered at 1.2 and 3.1 ppm, that reveal the presence of two types of OH. On the basis of available data for $AlPO_4$, the signal at 3.1 ppm can be assigned to tetrahedral P–OH groups. On the other hand, the signal at 1.2 ppm can be ascribed to Mg–OH groups. The solid calcined at 773 K gave three signals in the ^1H MAS spectrum, viz., the previous two and a third one centered at -0.1 ppm. This confirms that the structure of the material still contained some amorphous phase. On the basis of its upfield shift, the signal at -0.1 ppm can be ascribed to "basic" Mg–OH groups.

Finally, Fig. 9 shows the ^1H MAS NMR spectra for the $Mg_{100-x}P_x$ systems. Calcination of solid $Mg_{25}P_{75}$ at 623 K resulted in the appearance of signals at 1.2 and 3.1 ppm—the latter was a shoulder of the former and was better distinguished from the shape of the first ssb. These signals are thus consistent with those of amorphous magnesium described earlier; however, those for MgO were not observed owing to its low content in the sample. The solid remained amorphous on calcination at 773 K, consistent with the XRD and ^{31}P MAS NMR results; also, the spectrum was essentially identical with the previous one. The spectra for solid $Mg_{50}P_{50}$ were similar to the previous ones except that the signal at 5.2 ppm, corresponding to $Mg(OH)_2$, was apparent in the sample calcined at 623 K. The spectra for solid $Mg_{75}P_{25}$ exhibited well-defined signals for $Mg(OH)_2$; that at 5.2 ppm was the strongest in the spectrum for the uncalcined sample.

CONCLUSIONS

The results obtained in this work show that the synthesis of magnesium oxide–magnesium orthophosphate systems produces solids with separate MgO and $Mg_3(PO_4)_2$ phases. Calcining the solids has major effects on their structure, as does the MgO content (which increases the crystallization temperature of magnesium orthophosphaste). The ^{31}P NMR results confirmed the XRD findings. The former technique allows the proportions of crystalline and amorphous phases present in solids calcined at different temperatures to be quantified. Also, ^1H MAS NMR provides qualitative information on the nature of surface proton sites active in acid–base catalytic processes.

ACKNOWLEDGMENTS

The authors express their gratitude to the Spanish DGICyT for financial support awarded for the realization of this work as part of Project

PB92-0816 and to the staff of the Nuclear Magnetic Resonance Service of the University of Córdoba for their invaluable assistance in recording the NMR spectra.

REFERENCES

1. J. M. Campelo, A. García, D. Luna, and J. M. Marinas, *J. Catal.* **110,** 106 (1988).
2. J. B. Moffat, *in* "Topics in Phosphorus Chemistry" (M. Grayson and E. J. Griffith, Eds.), Vol. 10, p. 285. Wiley, New York, 1980.
3. J. M. Campelo, A. García, D. Luna, and J. M. Marinas, *J. Catal.* **102,** 299 (1986).
4. J. B. Peri, *Discuss. Faraday Soc.* **52,** 55 (1971).
5. T. Sakamoto, M. Egashira, and T. Seiyama, *J. Catal.* **16,** 407 (1970).
6. T. Seiyama, M. Egashira, T. Sakamoto, and I. Aso, *J. Catal.* **24,** 76 (1972).
7. M. Ruwet, P. Ceckiewicz, and B. Delmon, *Ind. Eng. Chem. Res.* **26,** 10 (1987).
8. J. B. Moffat and J. F. Neeleman, *J. Catal.* **31,** 274 (1973).
9. M. Giorgini, M. Bartolozzi, F. Morelli, and A. di Manno, *Ann. Chim.* (*Rome*) **65,** 29 (1975).
10. M. Coudurier, M. V. Mathieu, M. Prettre, B. Imelik, and M. E. Degeorges, *Bull. Soc. Chim. Fr.* 1821 (1968).
11. M. A. Aramendía, V. Borau, C. Jiménez, J. M. Marinas, and F. J. Romero, *J. Colloid Interface Sci.* **179,** 290 (1996).
12. M. A. Aramendía, V. Borau, C. Jiménez, J. M. Marinas, F. J. Romero, J. A. Navío, and J. Barrios, *J. Catal.* **157,** 97 (1995).
13. C. Dorémieux-Morin, C. Martin, J. M. Brégeault, and J. Fraisard, *Appl. Catal.* **77,** 149 (1991).
14. V. M. Mastikhin, U. V. Terskikh, O. B. Lapina, S. V. Filimonova, M. Seidl, and H. Knözinger, *Solid State NMR* **4,** 369 (1995).
15. L. Jhansi Laksmi, S. T. Srinivas, P. Kanta Rao, A. V. Nosov, O. B. Lapina, and V. M. Mastikhin, *Solid State NMR* **4,** 59 (1995).
16. M. Feike, R. Graf, I. Schnell, C. Jäger, and H. W. Spiess, *J. Am. Chem. Soc.* **118,** 9631 (1996).
17. P. Hartmann, C. Jana, J. Vogel, and C. Jägel, *Chem. Phys. Lett.* **258,** 107 (1996).
18. C. S. Blackwell and R. L. Patton, *J. Phys. Chem.* **88,** 6135 (1984).
19. J. Tropp, N. C. Blumenthall, and J. S. Waugh, *J. Am. Chem. Soc.* **105,** 22 (1983).
20. T. Kanazawa, T. Umegaki, and H. Kawazoe, "Proceedings of the 1st International Congress on Phosphorus Compounds," p. 107, IMPHOS, Rabat, 1977.
21. A. Pines, M. G. Gibby, and J. S. Waugh, *J. Chem. Phys.* **59,** 569 (1973).
22. S. R. Hartmann, and E. L. Hahn, *Phys. Rev.* **128,** 2042 (1962).
23. F. Brunet, and T. Schaller, *Am. Miner.* **81,** 385 (1996).